Enhancing the Energy Utilization of Hybrid Renewable Energy Systems

Yasser E. Abu Eldahab *, Naggar H. Saad **, Abdalhalim Zekry ***

* Electrical Power and Machines, Faculty of Engineering, Ain Shams University, Ph.D. Researcher, Cairo, Egypt

** Electrical Power and Machines, Faculty of Engineering, Ain Shams University, Professor, Cairo, Egypt

*** Electronics and Communications, Faculty of Engineering, Ain Shams University, Professor, Cairo, Egypt

(eng_yaser_hoseny@yahoo.com, naggar_hassan@yahoo.com, aaazekry@hotmail.com)

*Corresponding author Yasser E Abueldahab, eng_yaser_hoseny@yahoo.com, Cairo, Egypt, 00201069470245

Received: 13.11.2020 Accepted:13.12.2020

Abstract- Without question combining two or more renewable energy sources (RES) in hybrid topology can increase the overall system reliability and efficiency especially if they have a complementary nature. However, most RES has an intermittent nature of energy production due to dependency on weather conditions. Therefore, there are big challenges for coordinating between multiple sources of energy to optimize energy utilization. Therefore, this paper introduces a genetic algorithm (GA) based energy management and optimization method for Hybrid Renewable energy Systems (HRES). The proposed technique aims to determine the optimum share of power generation of each source so that minimizing the energy cost and emission and prolonging the battery lifetime. The proposed technique has been tested with an HRES system consists of Solar PV, Wind Generator, and Battery storage. different operating conditions of temperature, Irradiance, Wind speed, Battery status have been considered and tested. Also, the proposed method regards environmental and economical optimization and system reliability and security. The paper introduces the mathematical model of system components and compared the obtained results of simulation work and experimental work for validation under different operating conditions including real temperature, irradiance, wind speed, load profile for 24 hours.

Keywords Hybrid *R*enewable energy systems; Solar PV; Wind energy conversion systems, GA. Particle swarm PS.

Nomenclature

Abbreviations		α_i	The temperature coefficient of I_{sc}
ACO	Ant colony optimization	T_e	Electromagnetic torque
ASC	Genetic Algorithms	P_m	The mechanical power of the wind turbine
ATC	Annual total cost	I_L	The terminal current (A).
GA	Genetic algorithm	I_{ph}	The solar cell photocurrent(A).
GUI	Graphical User Interface	I_{SD}	The diffusion and saturation current (A)
MPPT	Maximum power point tracking	V_L	The terminal voltage (V).
NPV	Net present Value	R_s	The series resistance (Ω).
PMSG	Permanent Magnet Synchronous Generator	R_{sh}	The shunt resistance (Ω).
PSO	Particle Swarm Optimization	n	The ideality factor.
PV	Photovoltaic	K	Boltzmann's constant ($J.K^{-1}$).
RES	Renewable Energy Sources	q	The electronic charge (e)
SOC	Sate of charge	T	Solar cell temperature in kelvin (K)
TC	Total Cost	I_D	The diode current (A).
TSR	Tip Speed Ratio	I_s:	The series resistance current (A).
WTE	Wind Turbine Emulator	I_{sh}	The shunt resistance current (A).
Symbols		ρ	Air density
K_v , K_i	Proportional factors of typical values in ranges of (0.75-0.85) and (0.9-0.92) respectively.	ß	Blade pitch angle
θ_e	electrical angle	R	Turbine radius

$i_d, i_q, V_q, V_d, L_d, L_q$	The currents, voltages, and inductances of the d and q axis of PMSG	C_p	Power coefficient
Y_i	The lifetime year of ith HRES component	λ	Tip speed ratio
C_{cap_i}	The capital cost of the ith HRES component	v	wind speed
Φ	is the produced magnetic flux	I_a	Armature current
C	proportionality constant	I_f	Field current
E_{an}	The annual energy supplied by the ith HRES component	V_s	The supplied DC voltage
C_{cap_bat} , Y_{bat}	Capital cost and a lifetime of the battery source	E_A	The EMF induced voltage
C_{cap_w} , Y_w	Capital cost and a lifetime of WTE source	R_A, R_s	The armature and series resistances
C_{cap_pv} , Y_{pv}	Capital cost and a lifetime of PV source	R	Stator winding resistance
		P	Number of pole pairs
		α_v	The temperature coefficient of V_{OC}

1.Introduction

The last global status report of 2019[1] and the international electrical agency report of 2019[2] show that the wind and solar energy statistics have the highest growth rate and largest installation capacity. Besides, the Authors of [3] conducted a comprehensive review of a couple of hundreds of recent researches on HRES. They reviewed this bulk of researches on HRES in addition to applying a statistical and data mining analysis to extract frequent pattern sets which concluded the most utilized HRES combination and the most efficient optimization methods as regards reliability, economics, and the environment as listed in table 1. It shows that combining two or more RES in hybrid topology can significantly increase the total efficiency and reliability especially when they have complementary nature. Besides, it showed that wind, solar energy, and battery compile the best combinations of HRES as regard to the total power production and system reliability since solar and PV can complement each other. However, there are big challenges for coordination between these combined sources due to the intermittent nature of energy production i.e. system reliability and security. Therefore, optimizing the utilization of the output energy and synchronizing between different components of HRES is very essential for maximizing the total power production and satisfying the load requirements in addition to environmental, and economical optimization. Also, the survey concluded that the Genetic Algorithm (GA) and particle swarm (PSO) are the most efficient optimization algorithms for HRES. It shows the Loss of power supply possibility (LPSP) is the most efficient method for assessing and optimizing the reliability of HRES. Besides, the Levelized cost of energy (LCOE) is the most efficient for economical optimization.

Table 1 list of the HRES recommendations based on a comprehensive review in [3]

HRES	Tools	Optimization method	Reliability Method	Economical Method	Environmental method	Topology
Wind PV Battery	MATLAB	GA PSO	LPSP	LCOE	CO2	Standalone DC-Bus

On the other hand, many research contributions have been introduced for developing the optimization of HRES. For example, the authors of [4] presented a model of HRES consists of PV, Wind, and Battery in standalone topology. They ran Net present Value (NPV) based on economical optimization. They utilized the Big Bang Big Crunch (BBBC) optimization method for utilizing the system operation. Their work has been modeled and simulated using MATLAB Simulink. also, the Authors of [5] introduced an HRES model consists of PV, wind, Diesel, and Battery in standalone topology and conducted economical optimization based on the NPV technique. They simulated their model by using MATLAB. Furthermore, the authors of [6] presented a standalone HRES which is composed of PV, Wind, and Battery. Their proposed model was economically optimized by using the Total cost (TC) technique and operation was optimized by utilizing GA and Exhaustive Search Technique (ES) algorithms. Furthermore, another HRES model consists of PV, Battery, and Wind has been developed and simulated in [7]. The authors designed their model in standalone topology and ran economical optimization based on the TC technique. And they optimized the operation by using Ant Colony (ACO). They utilized MATLAB Simulink to simulate their mathematical model. Also, the authors of [9] performed a comparison between PSO and TS optimization methods on an HRES model which consists of PV, Wind, and Battery in standalone topology. They also applied the Annual cost (ACS) method for economically optimizing the proposed model. They used MATLAB Simulink in simulating their proposed system. Furthermore, in [10], the authors compiled an HRES model by combining PV, Wind, and battery in standalone. They utilized a TC method in economical optimization and applied the Cumulative Savings (CS) method for optimizing the utilization of the generated power. Moreover, authors of [11] formed HRES consists of PV, Wind, and Diesel in standalone topology. They economically optimized their proposed HRES by using the TC method and optimized the utilization based on GA and MARKOV. They used MATLAB Simulink in simulating their work. Besides, an HRES system has been introduced in [12] which is composed of PV, Wind, Diesel, and battery in standalone topology. They utilized the Discrete harmony search (DHS) method in optimizing the utilization and Total Annual Cost (TAC) in performing economical optimization. Furthermore, the Method of TAC economical optimization and PSO optimization technique has been utilized for the proposed HRES in [13]. The proposed model consists of PV, Wind, and battery in standalone topology. Also, authors of [14] developed standalone topology-based HRES by combining

PV, Wind, Battery, and Supper capacitor. They economically optimized their system by applying the TC method and optimized power utilization based on GA. They also managed system reliability based on LPSP. For summing up the previous review, these researches concluded helpful recommendations by which researchers can be guided to choose the suitable control and optimization techniques for their prospective systems. However, all these researches have been conducted on specific configurations and sizes of HRES components which were designed beforehand. Therefore, their conclusions and recommendations are valid and helpful only for typical or identical cases of their designs, specifications, and configurations of HRES components and they have a big risk on system security and reliability. Consequently, there is still a knowledge gap in having smart energy management and utilization method for determining the optimum share of each power source of HRES based on the weather conditions i.e. Temperature, Irradiance, Wind Speed, Depth of discharge (DOD), state of charge (SOC) in addition to priority of economic, environmental, and reliability requirements. This paper presents GA based energy management and utilization technique. The proposed method receives the user request of priority of environmental and economical requirements, measurements of temperature, wind speed, Irradiance, battery status of charging and discharging, and then it interprets these pieces of information into commands for driving the system to produce the optimum share of each power source of HRES so that it minimizes the total energy cost and emission and prolonging battery life. The paper introduces all mathematical models of HRES components i.e. Solar PV, Wind, and battery in addition to the optimization method. The simulation work has been done by using MATLAB Simulink. Besides, it presents the experimental prototype of HRES including the proposed method based on an Atmel 8-bit AVR microcontroller. The rest of the paper is organized as follows: Section 2 presents all HRES components, and the proposed optimization method; section 3 discusses the results; section 4 concludes the work.

2. Methods

The proposed HRES model is composed of solar PV modules, Wind Turbine, and Battery. Therefore, this section introduces the mathematical model of each system component. a Wind turbine emulator (WTE) has been developed based on coupling separately excited DC motor with speed drive to play the role of the wind generator. It is utilized in simulation and experimental work to imitate the Wind Turbine and coupled with a permanent magnet synchronous generator (PMSG) to emulate a complete wind energy conversion system (WECS). Also, the proposed system includes a new MPPT technique for optimizing the generation of PV and Wind energy systems based on integrating particle swarm with the binary search algorithm. Also, it includes a new optimization method for utilizing the output generated power based on economical and environmental requirements as well as operating conditions. All these methods will be presented in this section.

2.1 System Description

As shown in Fig. 1, the proposed HRES is composed of PV, WTE, and Battery. The PV is connected to the common DC bus through the Boost converter. the WTE is connected to the common DC bus through a rectifier and boost converter. And the battery is bidirectionally connected to the common DC bus through a Buck-Boost converter. The system can supply the DC load, AC load, and export it to the grid as well. In the following subsections, all components of the proposed model will be presented in detail.

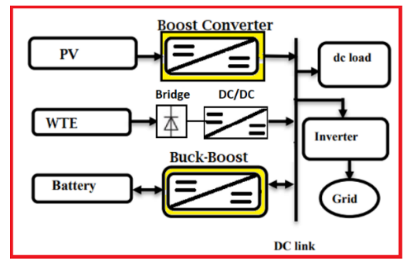

Fig. 1 The proposed HRES Block Diagram

2.2 PV model:

The most practically used models of solar PV, are the single and double diode models. The single diode model is more used for modeling a large PV system while the double diode model is used when taking into consideration the recombination effect [4,15]. The single Diode model is used in the proposed system.

2.2.1 Single diode model

Fig. 2 shows the equivalent circuit of the single diode model and its model equations [15,16] are as follow

$$I_L = I_{ph} - I_{SD}\left(e^{\left(\frac{q(V_L + I_L R_s)}{nKT}\right)-1}\right) - \left(\frac{V_L + I_L R_s}{R_{sh}}\right) \qquad (1)$$

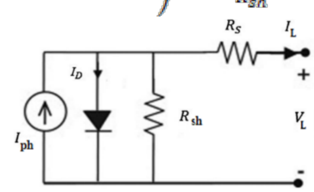

Fig. 2. PV single diode model.

By applying the model equations above in MATLAB/SIMULINK, Fig.3 shows the general PV model integrated with the Boost converter and the newly proposed MPPT technique. Also, it shows the ability to set the module parameters like open circuit voltage, short circuit current, temperature coefficients of open-circuit voltage, and short circuit current so that it can emulate a wide range and capacities of PV modules.

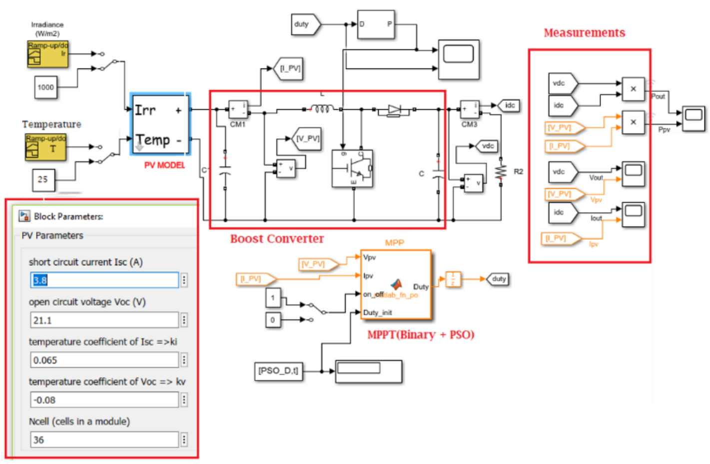

Fig. 3 General PV model integrated with the new MPPT and Boost converter.

2.3 The WECS Model

This section introduces the mathematical model of all components of the WECS as well as presenting the experimental prototype components and the working principles of the proposed system.

2.3.1 Wind Emulating energy conversion system modeling

Fig. 4 shows the block diagram of the proposed wind emulator integrated with the generation unit. It is composed of MPPT based Torque signal generator control system, a Wind turbine emulating unit which is composed of a series type DC motor with a DC drive, and PMSG.

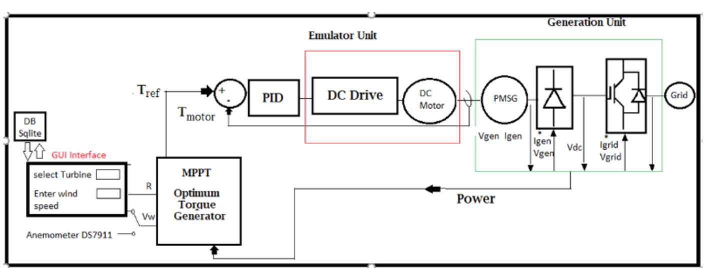

Fig. 4 The System Block diagram

On the other hand, fig. 5 shows the generation sub-model which is coupled with the DC motor-based wind emulator model. It also includes the power electronics subsystems including rectifying, converting, and inverting sections. As shown in Fig. 5, the sub-model consists of the model of the PMSG, universal bridge that rectifies the AC output of the generator to DC voltage, DC link, Diodes based universal bridge rectifier. PWM IGBT inverter, LC filter, and measurement devices. The DC motor speed and torque are controlled so that the coupled generator produces the maximum power.

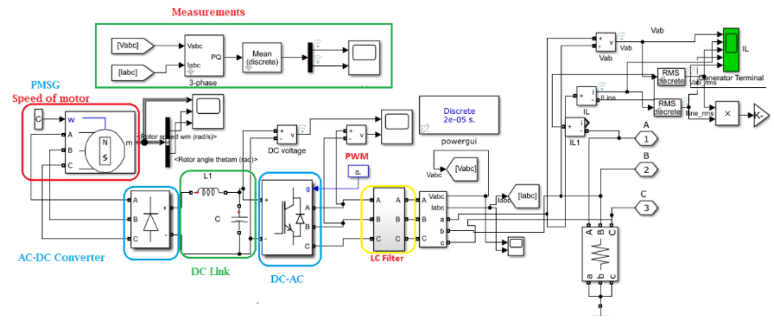

Fig. 5 The Model of the generator coupled with the controlled DC motor

2.3.4 The WTE System prototype

Fig. 6 shows the block diagram of the system prototype circuitry. It is based on an Atmel 8-bit AVR microcontroller that receives analog signals of current and voltages of generator and grid output signals, DC link voltage as well. Also, it receives the torque signal of motor generator coupling. It is responsible for calculating the generated power and calculating the reference torque and speed. Also, it generates switching pulses for motor drive, converter, and inverter at generation and grid side. Besides, the system includes a series of excited DC motor and PMSG. Furthermore, it includes an LCD that displays 2 lines of 16 characters for showing system metrics. Also, the system includes many sensing and measurement devices i.e. current and voltage sensors 0-10 VDC, Anemometer DS7911.

2.3.5 philosophy of operation of the WTE

The microcontroller receives the turbine attributes and the sensed wind speed and direction by utilizing an anemometer sensor DS7911. It then searches the database to fetch the optimum Tip Speed Ratio (TSR) thanks to the new MPPT proposed technique. Besides, it calculates the optimum torque based on the feedback power signal and the pivot speed so that, the system can generate the maximum power. The controller generates switching pulses based on the driving reference signals of torque and speed and applies them to the motor drive as commands. Besides, it generates the switching pulses for driving the power switches in rectifier and inverter circuits. Furthermore, the microcontroller sends all metrics of measured parameters like rotating speed, torque, current, voltage, and power values to the serial port to enable users to monitor system parameters throughout the operation rather than displaying the most important metrics on the LCD screen. Furthermore, the controller enables the pitch control by tuning the motor speed based on the received feedback of the power signal. If the power is going to exceed the rating power, the controller would reduce the motor speed so that generator works
within the limits of its power rating. Table 2 lists the bill of material (BOM) including components of the proposed prototype.

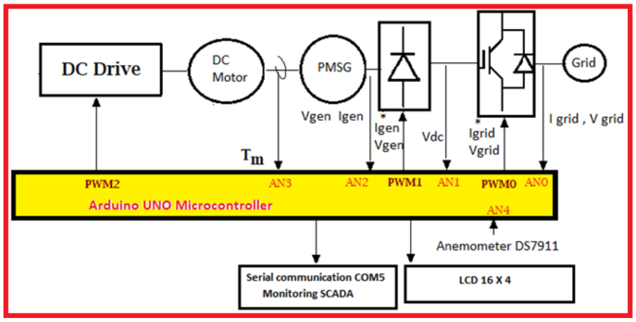

Fig. 6 Block Diagram of the proposed WTE prototype

Table 2 The BOM of the proposed wind emulator

Component	Description	Count
DCM	DC motor of 250W power rating, Supply voltage 12VDC, Speed up to 15000RPM	1
PMSG	Permanent magnet miniature generator of 250W, 50HZ,220v, and 0.85 power factor, speed range1500-10000 RPM	1
Battery 12v - 100AH	12V Battery of 100AH capacity	1
SQL 50A 1000v	Three-phase bridge rectifiers of 50A and 1000V rating.	1
L9110	Dual motor speed drive	1
Speed sensor	Motor shaft encoder	1
LCD1604	LCD 16 X 2	1
Arduino UNO R3	Atmel 8-bit AVR microcontroller	1
DS7911	Anemometer for measuring wind speed and direction	1

2.3.6 The new MPPT for PV and Wind emulator

A new MPPT method has been developed for maximizing the extracted power of PV and Wind energy systems in addition to the main objective which is optimizing the utilization of the generated power. It utilizes a binary search technique combined with the PSO algorithm to fetch the target MPP accurately and so fast as some approach is presented in [17].

2.3.6.1 Objective function and constraints

This method services in two subsystems the PV and Wind. Therefore, it has two versions of multiple objective functions for both systems. Starting with the PV subsystem, by measuring the current and voltage of PV modules, it is found that the optimum current is proportional to the short circuit current and similarly the optimum voltage is proportional to the open-circuit voltage [18]. Therefore, the given equations below can be used in determining the optimum power as follows:

$$I_{optimum} = K_i * I_{sc} \tag{2}$$

$$V_{optimum} = K_v * V_{oc} \tag{3}$$

With,

$$I_{SC} = I_{SCs}\,(G/G_s) + \alpha_i\,(T - T_s) \tag{4}$$

$$V_{OC} = V_{OC_S} + \alpha_v\,(T - T_S) - (I_{SC} - I_{SCs}) \tag{5}$$

With constraints:

$$0 \le I_{optimum} \le I_{sc}$$

$$0 \le V_{optimum} \le V_{oc}$$

Similarly, for the wind subsystem, the wind turbine mechanical power can be represented as follows [19]:

$$P_m = \frac{1}{2}\rho\pi R^2 v^3 C_p(\lambda,\beta) \tag{6}$$

The power coefficient represents the efficiency of extracting the power of a wind turbine. It is a nonlinear function of the blade pitch angle β and the tip speed ratio λ and can be written as:

$$C_p(\lambda,\beta) = 0.5\left(116\frac{1}{\lambda_i} - 0.4\beta - 5\right)e^{-(21/\lambda_i)} \tag{7}$$

with

$$\frac{1}{\lambda_i} = \frac{1}{\lambda+0.08\beta} - \frac{0.035}{1+\beta^3} \tag{8}$$

Where the tip speed ratio expresses the relation between the rotor speed w_m to the wind speed v_w as follows:

$$\lambda = w_m R/v_w \tag{9}$$

2.3.6.2 Principle of operation

Fig. 7 shows an example of the operation scenario and Fig. 8 charts the logic flow. The target MPP should be at point 4 and operation starts at point 1. The nearest point to the target is point 2 which is determined accurately, thanks to the PSO technique. Then it starts from point 2 and applies the binary search algorithm by dividing the search range into two parts and checking the slope of $\frac{dp}{dw}$ in the middle of the range at point 3 to decide the direction and update the start and the endpoints of the new search range. Consequently, one part is discarded, and the other part is taken as the new search space. Again, it divides the new search domain into two parts and checks the slope of $\frac{dp}{dw}$ at the middle point. The process is repeated until the target is reached which is at point 4 in this example. The obtained point is stored in the Database; besides, it is forwarded to the motor drive controller as a reference speed. It is noticed that the target point has been reached in few iterations while takes thousands of iterations in conventional methods i.e. perturb and observation (P & O) method.

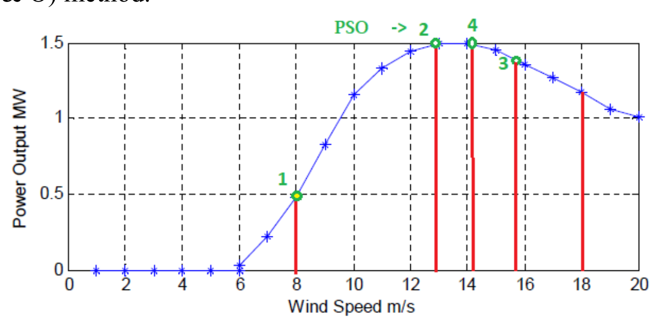

Fig. 7 Example of the proposed MPPT tracking steps

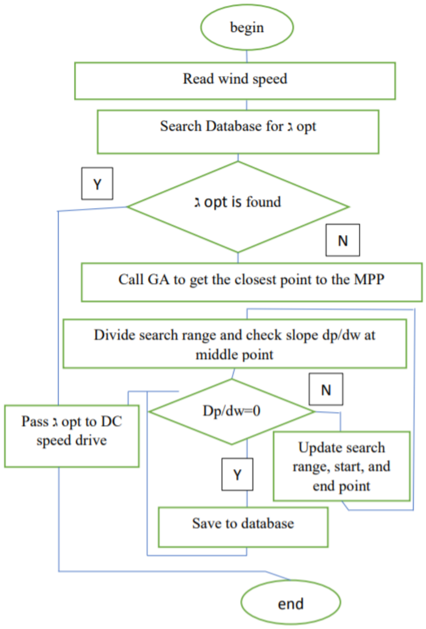

Fig. 8 Flowchart of the proposed MPPT speed control method

2.4 The proposed optimization of power utilization

Optimizing the utilization of the generated power of HRES is the main objective of the proposed model. The optimization process has considered the economic and environmental requirements with all respect to the system security for satisfying load demands and all system constraints. Fig. 9 shows the block diagram of the proposed optimization process. It shows the inputs and proposed outputs of the process. It has been developed based on the GA algorithm by accepting inputs of the operating conditions i.e. Wind speed and direction profile, irradiance, and temperature profile as well. Also, it gets the load profile to be considered in load dispatch calculations. It also receives the operating time for considering working on-peak or off-peak duration. Furthermore, it gets the battery voltage and SOC to decide for charging, discharging, or disconnecting the battery. Furthermore, it receives the environmental and economical user priority requests. It then applies the GA algorithm considering all system constraints to determine the share and weight of the generation of the PV, Wind, Battery, and Grid power. The outputs are in form of switching pulses with a specific frequency and duty cycle which are forwarded to the related control circuit of each subsystem. The full list of all objective functions and system constraints of the proposed technique are listed below thanks to some researches on environmental and economical optimization conducted in [20-27].

Inequality constraints

$$0 \le P_{Pv} \le Ppv_{max} \quad (10)$$
$$0 \le P_{W} \le Pw_{max} \quad (11)$$
$$0 \le P_{bat} \le Pbat_{capacity} \quad (12)$$
$$SOC_{min} \le SOC \le SOC_{max} \quad (13)$$
$$V_{cut-off} \le Vbat \le V_{fullcharge} \quad (14)$$
$$Ibat_{max\_charge} \le Ibat \le Ibat_{max\_discharge} \quad (15)$$
$$-(Ppv + Pw - Pbat - P_{Load}) \le Pgrid \le P_{Load} \quad (16)$$

Equality constraints

- With no considerations of losses
$$P_{Load} = Ppv + Pw + Pbat + Pgrid \quad (17)$$
- With losses consideration
$$P_{Load} = Ppv + Pw + Pbat + Pgrid - P_{Losses} \quad (18)$$
- Case of battery at cutoff voltage:
$$P_{Load} = Ppv + Pw + Pgrid - P_{Losses} \quad (19)$$

Objective functions:

The optimization of power utilization has considered the environmental and economical optimization with complete fulfillment of load requirements based on load following dispatching approach. The objective function will be as follows:

$$\min LCOE \sum_{i=1}^{n} \frac{\frac{C_{cap_i}}{Y_i}}{E_n} = \frac{\frac{C_{cap\_pv}}{Y_{pv}} + \frac{C_{cap\_w}}{Y_w} + \frac{C_{cap\_bat}}{Y_{bat}}}{E_n} \quad (20)$$

The load dispatch has been evaluated based on LPSP as follows:

$$LPSP = \sum_{i=0}^{T} \frac{Power\ Failure\ time\ (P_{generation} \le P_{Demand})}{N} \quad (21)$$

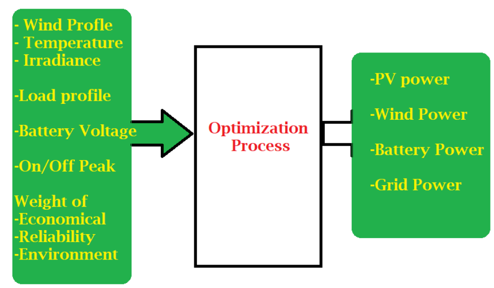

Fig. 9 The proposed optimization technique.

3. Results and discussion

This section presents the test results of simulation and experimental work of the HRES system including all components which are: PV modules with 250W, Wind generator of 250W, and battery of capacity 100Ah for supplying 1kW DC Load. The test of simulation and experimental work has been run on real data of Irradiance, temperature, wind speed profiles for 24 hours in Cairo the capital of Egypt on the 15th of September 2020 as shown in Fig. 10,11, and 12.

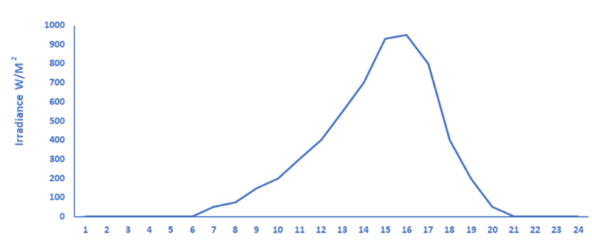

Fig. 10 Irradiance profile during 24 hours in Cairo on 15th of September 2020

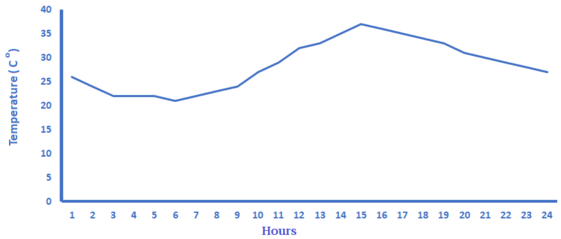

Fig. 11 Temperature profile during 24 hours in Cairo on 15th of September 2020

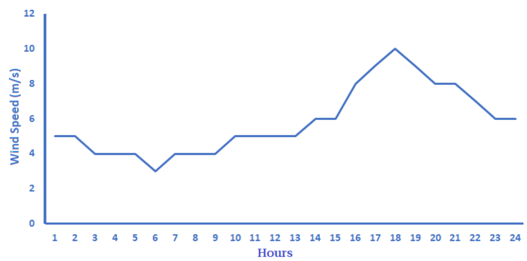

Fig. 12 Wind profile during 24 hours in Cairo on 15th of September 2020

3.1. **Testing the new MPPT algorithm**

In this test case, the system is tested under the control of a traditional P&O tracking algorithm and the new MPPT technique as well. Fig. 13 shows the results of the traditional P&O in the curve on the left side and the results of the new MPPT algorithm on the right. it is noticed obviously that, the new MPPT algorithm reaches the target MPP in few iterations while the conventional P&O takes hundreds of iterations to fetch the target point. Besides, the new algorithm minimizes the ripple and more accurate than the traditional technique.

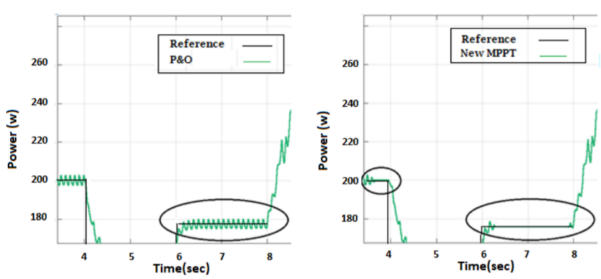

Fig. 13 Tracking the MPP by traditional and the new method

3.2.1 Testing the proposed optimization method

Fig. 14 shows the graphical statistics of the outputs of the GA tools showing the optimum values of the best individuals of the power generation weight of each component of the proposed HRES. It also shows the finesses of individuals, the best, and the mean fitness. Furthermore, it shows the criteria to stop conditions. Table 3 lists the values of the GA operators and parameters that are used in the test.

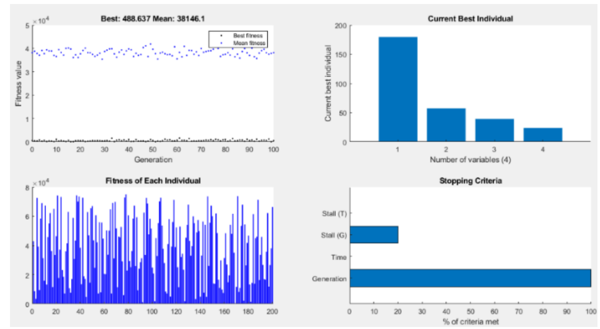

Fig. 14 The statistics of the GA based optimization technique

Table 3 The GA operators and parameters

Parameters/Operators	Value
Mutation Rate	0.05
Display	Final
Crossover Rate	0.8
Stall Generation limit	5
Number of Generations	100
Number of populations	200

Table 4 lists some test cases of the proposed optimization conditions including all input metrics and obtained results thanks to the proposed add-on feature of serial monitoring and data logging. It shows in test case 1 represented by the 1st row that, the PV and wind power were close to their maximum which is 250 W because temperature, Irradiance, and wind speed are at the standard condition which are 25℃, 1000 W/m^2 , 12 m/s respectively. Also, Battery and grid shared with the remaining required amount of power to satisfy the load while the grid share is higher than the battery due to operating at off-peak duration. So, the priority is given to Grid for saving Battery power to increase its lifetime and using the cheap energy price at an off-peak time. Furthermore, in the second test case represented by the second row, all test conditions are like that of case 1 but the operation was at the on-peak time. Therefore, the PV and Wind produced about their maximum power, but the grid did not share any power and the battery complemented the remaining of the demanded power to avoid the high price of energy at peak time. Besides, in test case 3, the battery did not share any power due to its voltage was at 8V which is below the cutoff voltage (9V). Furthermore, case 4 shows that when the irradiance was 500 W/m^2 . Therefore, the PV power was reduced to about half of its capacity. Besides, test case 5 shows that, when wind speed was at cutoff speed (2 m/s), there was no power produced from the WTE. Also, case 6 Shows the charging of the battery when wind and/or PV power exceeded the demanded power. Furthermore, case 7 shows that there is no charging of the battery due to battery voltage is equal to the full charge voltage (14.1v). Moreover, case 8

Table 4 Different test cases of the optimization method

#	TEMPE RATURE ℃	IRRADIA-NCE W/m^2	WIND SPEED m/s	POWER LOAD (W)	BATTERY VOLTAGE (V)	PEAK TIME	ECONO-MICAL	RELIA-BILITY	ENVIRON-MENTAL	POWER PV (W)	POWER WIND (W)	POWER BATTERY (W)	POWER GRID (W)
1	25	1000	12	1000	10	OFF	YES	YES	NO	**240.65**	**228.14**	**11.79**	**519.42**

2	25	1000	9	1000	10	ON	YES	YES	NO	**246.17**	**237.5**	**516.33**	**0**
3	25	1000	11	1000	8	ON	YES	YES	NO	**243.15**	**233.85**	**0**	**523.09**
4	25	500	10	1000	9	OFF	YES	YES	NO	**127.77**	**228.56**	**10.1**	**633.50**
5	25	1000	2	1000	12	OFF	YES	YES	NO	**233.21**	**0**	**94.22**	**672.50**
6	25	1000	9	300	10	ON	YES	YES	NO	**246.17**	**237.5**	**0**	**-180.01**
7	25	1000	11	450	14.1	OFF	YES	YES	YES	**249.99**	**200.99**	**0**	**0**
8	25	1000	11	1000	13	OFF	NO	YES	YES	**249.99**	**249.99**	**500**	**0**
9	25	1000	3	1000	12.5	ON	YES	YES	NO	**249.99**	**83.33**	**666.67**	**0**

shows that, despite operation is at an off-peak time, the grid did not share any power due to environmental priority is requested by the operator. And battery complemented the remaining power to satisfy the load. Besides, case 9 showed a reduction in Windpower due to working at low wind speed.

3.2.2 Simulation test results

3.2.2.1 Economical and reliability test case

Fig. 15 shows the power of the load in yellow, PV in dark brown, Grid in light brown, the battery in green, and wind in violet-colored line respectively. It represents the case when economics and reliability are given priority for 24 hours of supplying the load. It shows that PV and Wind complement each other. Besides, the load power is followed and fulfilled as long as the whole test duration. Furthermore, the Battery is invoked at peak hours' time (7 pm-11 pm).

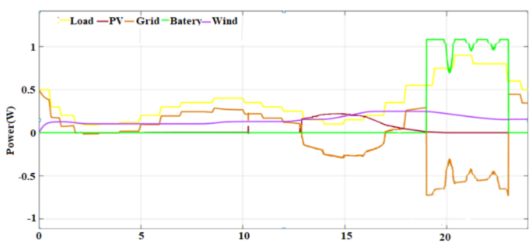

Fig. 15 Simulation results of Economical and reliability test case

3.2.2.2 Environmental and reliability test case

Fig. 16 shows the power of the load in dark brown, PV in light brown, Grid in violet, the battery in green, and wind in blue colored line respectively. It represents the case of when environment and reliability are given priority for 24 hours of supplying the load. It shows that Battery has the priority above the grid as long as it has power. Besides, the Battery is off when its voltage goes down the cut off voltage and the Grid complements the missing amount of power to fulfill the load demand. Also, the battery is charging when the wind and or the PV power exceed the load demand. Furthermore, it shows that excessive power is exported to the GRID represented in the negative part of the Grid Power curve.

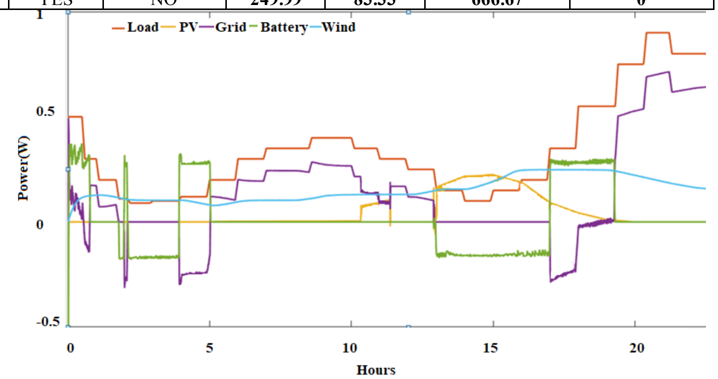

Fig. 16 Simulation results of combining Environmental and reliability test case

3.2.2.3 Testing combinations of Grid and PV sources

Fig. 17 shows the case of combining PV with Grid to feed the load. It shows the Grid supplies when absent of sun and vice versa. Furthermore, it shows the power exported to the Grid when PV power exceeds the demanded power.

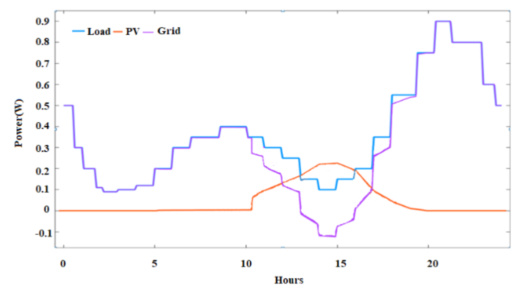

Fig. 17 Simulation results of combining Grid and Wind test case

3.2.2.4 Testing combinations of Grid and PV sources

Fig. 18 shows the case of combining Wind with Grid to feed the load. It shows the Grid supplies when absent of wind power and vice versa. Furthermore, it shows the power exported to the Grid when the Windpower exceeds the demanded power.

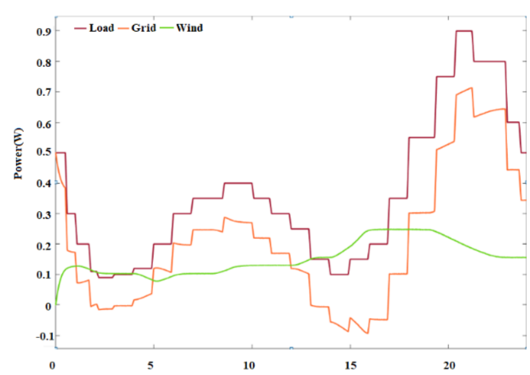

Fig. 18 Simulation results of combining Grid and Wind test case

3.2.2.5 Testing combinations of Grid, Wind, and PV sources

Fig. 19 shows the case of combining Wind, PV, and the Grid to feed the load. It shows the Grid complements the missing power to fulfill the load. Furthermore, it shows the power exported to the Grid when the sum of Wind and PV power exceeds the demanded power.

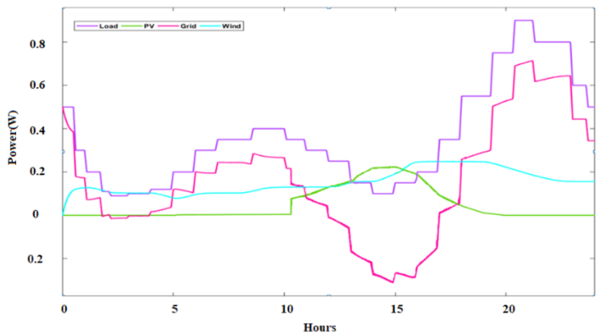

Fig. 19 Simulation results of combining Grid, Wind and PV test case

3.2.2.6 Testing combinations of Grid, Win, and Battery sources

Fig. 20 shows the case of combining Wind, Battery, and the Grid to feed the load. It shows the battery complement the missing power to fulfill the load as long as there is the power inside. Besides, it stops supplying when its voltage goes under the cutoff voltage and the Grid takes the mission. Also, it shows the power exported to the Grid when there is excessive power.

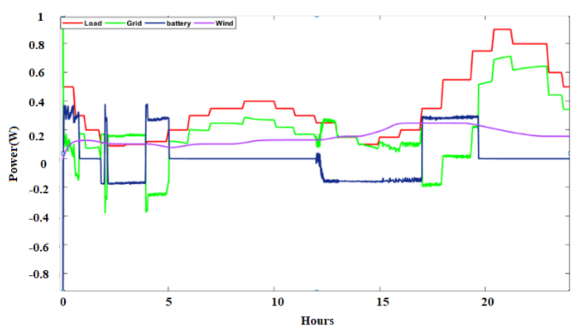

Fig. 20 Simulation results of combining Grid, Wind, and Battery test case

3.2.2.7 Testing combinations of Grid, PV, and Battery sources

Fig. 21 shows the case of combining PV, Battery, and the Grid to feed the load. It shows the battery complement the missing power to fulfill the load as long as there is a power inside. Also, it stops supplying when its voltage goes under the cutoff voltage and the Grid takes the mission. Also, it shows the power exported to the Grid when there is excessive power.

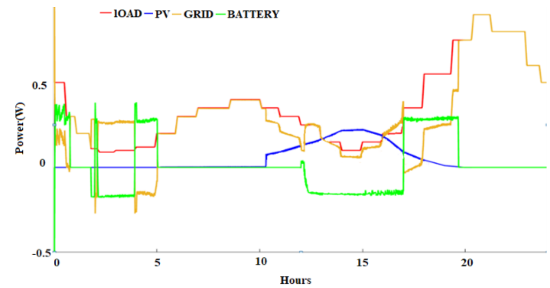

Fig. 21 Simulation results of combining Grid, PV, and Battery test case

3.2.2.8 Comparison between all HRES combination as regard Grid power consumption and exporting

Table 5 lists the statistics i.e. minimum, maximum, mean, median, and standard deviation (STD) of the Grid power of all cases of combinations of HRES components. Besides, Fig. 22 compares the Grid power curves of all HRES combinations, they show that the combination of PV, Wind, Battery, and Grid is the best in exporting power to the Grid and the least one in Grid power consumption. Besides, it shows that the worst combination as regard to grid power consumption is the combination of PV, Battery, and The Grid and the combination of Wind, Battery, and Grid, a combination of PV, Battery, and Grid, and combination of PV and Grid.

Table 5 Statistics of simulation results of Grid Power of All HRES Combinations

Case Statistics	PV, Wind, Battery, Grid	PV, Grid	Wind, Grid	PV, Wind, Grid	Wind, Battery, Grid	PV, Battery, Grid
Min (W)	-379.9	-125.7	-90	-313	90	-271.2
Max (W)	714.5	900	714.5	714.5	900	900
Mean	97.72	302.2	197.8	148.2	351.8	294.9
Median	0	272.2	169.5	116.4	300	288.3
Std	6.883	0.2713	0.2192	0.266	0.2318	0.2563

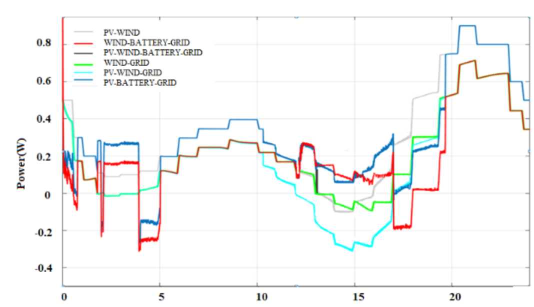

Fig. 22 Simulation results in comparison of grid Power of all HRES components combinations

3.2.3 Experimental test results

In this section, the experimental results are presented and discussed. The test cases include the economical and environmental optimization and comparing different combinations of HRES components as regard to the Grid consumption and the cases of exporting excessive power to the

Grid. Fig. 23 depicts the experimental schematics of the whole system showing the PV, Battery, WTE interfacing circuits.

3.2.3.1 Test case of economical and system reliability

Fig. 24 depicts the results of having all HRES components combined and the priority is given to the economical and reliability optimization. It shows that wind power and solar PV power are complementary sources. Besides, it shows the output power of the WTE at wind speed lower than the cut-in and over the cut-off wind speed as noticed in table 6,7 in the highlighted columns in yellow. It successfully governs the generators to work up to their power rating as shown in the blue colored line curve. Furthermore, it shows the Battery power represented by the brown line curve, it is invoked at peak duration (7 pm to 11 pm) to save the high price energy as clearly shown in table 8. Furthermore, it shows the grid only complements the missing power to fulfill the load demand of power and the exporting of power to the Grid when there is excessive power.

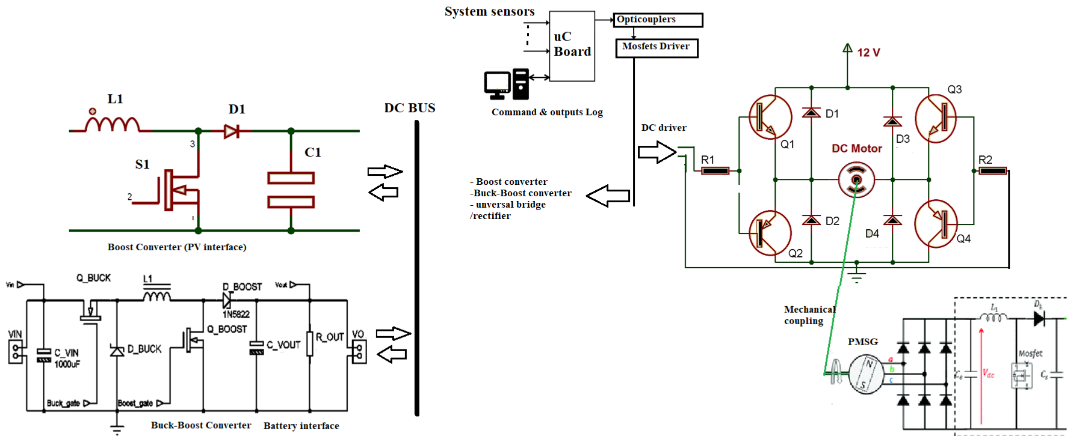

Fig. 23 Experimental circuit schematic of the proposed system.

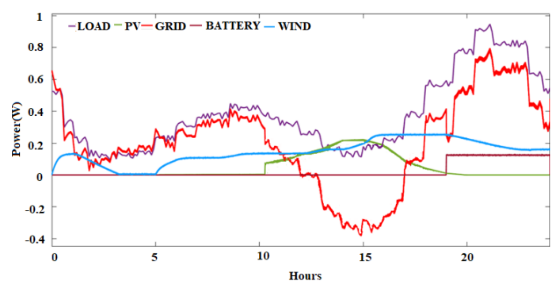

Fig. 24 Experimental test case of economical and reliability optimization.

Table 6 The wind power output at cut-in wind speed

Scan Cycle	Time (HH:MM: SS)	Temperature ℃	Irradiance W/m^2	Wind Speed m/s	V Battery (V)	Peak Time	economics	Reliability	Environment	Power Load (W)	Power PV (W)	Power Grid (W)	Power Battery (W)	Power Wind (W)
14399	3:59:59	22	0	1.182	12.101	off	Yes	Yes	No	130	0	162	0	0
14400	4:00:00	22	0	1.264	12.031	off	Yes	Yes	No	130	0	156	0	5
14401	4:00:01	22	0	1.146	12.098	off	Yes	Yes	No	130	0	162	0	0

Table 7 The wind power output at cut-off wind speed

Scan Cycle	Time (HH:MM: SS)	Temperature ℃	Irradiance W/m^2	Wind Speed m/s	V Battery (V)	Peak Time	economics	Reliability	Environment	Power Load (W)	Power PV (W)	Power Grid (W)	Power Battery (W)	Power Wind (W)
57600	16:00:00	35	800	11.903	11.732	off	Yes	Yes	No	233	163	-223	0	249
57601	16:00:01	35	799.889	11.513	11.648	off	Yes	Yes	No	233	164	-230	0	250
57602	16:00:02	34.999	799.778	11.417	11.451	off	Yes	Yes	No	233	166	-236	0	250

Table 8 The battery output during the on-peak period.

Scan Cycle	Time (HH:MM: SS)	Temperature ℃	Irradiance W/m^2	Wind Speed m/s	V Battery (V)	Peak Time	economics	Reliability	Environment	Power Load (W)	Power PV (W)	Power Grid (W)	Power Battery (W)	Power Wind (W)

75600	21:00:00	29	0	7	11.556	on	Yes	Yes	No	926	0	760	124	194
75601	21:00:01	28.999	0	6.999	11.521	on	Yes	Yes	No	926	0	757	125	195
75602	21:00:02	28.999	0	6.999	11.588	on	Yes	Yes	No	926	0	748	129	199

3.2.3.2 Test case of environmental and reliability.

in this test case, the priority is given to environmental and reliability optimization. Therefore, Fig. 25 depicts the line curves of all HRES power. It shows that the battery complements the missing power to fulfill the load as long as it has the power to reduce emissions due to using the Grid power as highlighted in yellow in Table 9. Also, it shows that the Battery stops supplying when its voltage goes under the cut-in voltage. Furthermore, it shows the exporting of any excess power to the Grid.

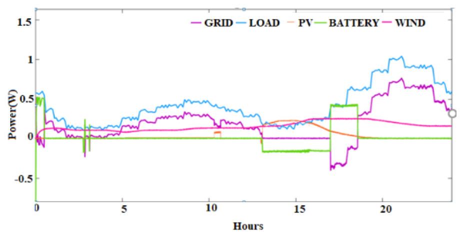

Fig. 25 Experimental test case of environmental and reliability optimization.

3.2.3.3 Test case of combining PV, Wind, and Grid

Fig. 26 shows the results of combining PV, Wind, and Grid, it shows that the Grid complements the missing power to fulfill the load while it absorbs any excessive power as highlighted in table 10.

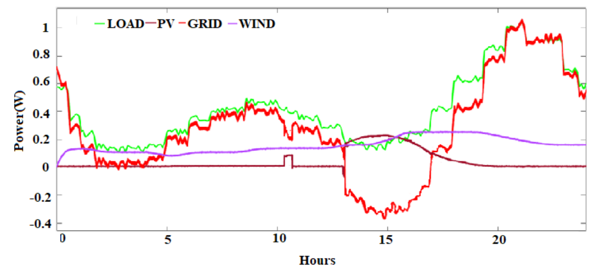

Fig. 26 Experimental test case of combining PV, Wind, and Grid

Table 9 The battery and grid power at off-peak while environmental optimization.

Scan Cycle	Time (HH:MM: SS)	Temperature °C	Irradiance W/m^2	Wind Speed m/s	V Battery (V)	Peak Time	economics	Reliability	Environment	Power Load (W)	Power PV (W)	Power Grid (W)	Power Battery (W)	Power Wind (W)
7200	2:00:00	22	0	4	12.313	off	Yes	Yes	Yes	118	0	0	55	74
7201	2:00:01	22	0	4	12.183	off	Yes	Yes	Yes	118	0	0	51	77
7202	2:00:02	22	0	4	12.118	off	Yes	Yes	Yes	118	0	0	44	83

Table 10 Exported excessive power to the grid

Scan Cycle	Time (HH:MM: SS)	Temperature °C	Irradiance W/m^2	Wind Speed m/s	V Battery (V)	Peak Time	economics	Reliability	Environment	Power Load (W)	Power PV (W)	Power Grid (W)	Power Battery (W)	Power Wind (W)
50400	14:00:00	37	930	6	12.646	off	Yes	Yes	No	119	212	-250	0	157
50401	14:00:01	37	930.006	6	12.709	off	Yes	Yes	No	119	210	-252	0	161
50402	14:00:02	36.999	930.011	6.001	12.755	off	Yes	Yes	No	119	207	-251	0	163

3.2.3.4 Test case of combining Battery and Grid

Fig. 27 depicts the results of combining Battery and Grid, it shows that the Grid supplies the load a hundred percent except at on-peak duration it shares the battery to fulfill the demanded power.

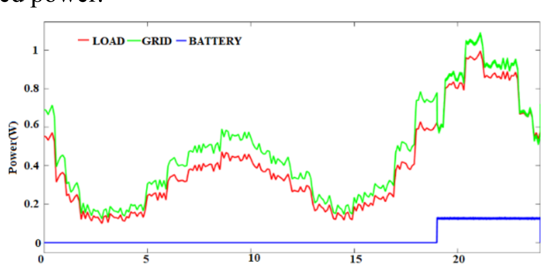

Fig. 27 Experimental test case of combining Battery and Grid

3.2.3.5 Test case of combining PV, Battery, and Grid

Fig. 28 depicts the results of combining PV, Battery, and Grid, it shows that the Grid complements the remaining power to fulfill the load on off-peak duration while the battery shares the Grid to complement the missing power for satisfying the demand requirements.

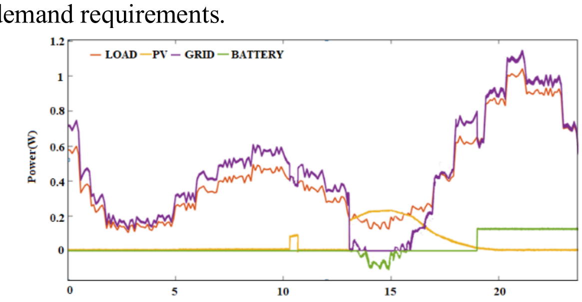

Fig. 28 Experimental test case of combining PV, Battery, and Grid

3.2.3.6 Test case of combining Wind and Grid

The test case depicted in Fig. 29 shows the combination of Wind and Grid. It shows that the Grid complements the missing power to fulfill the load. Also, it shows the exporting of any excess power to the Grid.

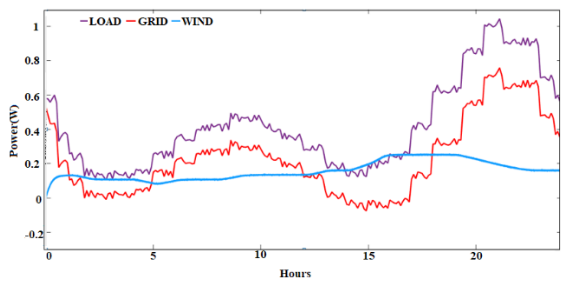

Fig. 29 Experimental test case of combining Wind and Grid

3.2.3.6 Test case of combining PV and Grid

The test case depicted in Fig. 30 shows the combination of PV and Grid. It shows that the Grid complements the missing power to fulfill the load. Also, it shows the exporting of any excess power to the Grid.

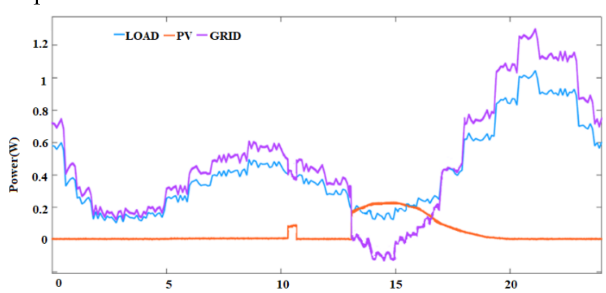

Fig. 30 Experimental test case of combining PV and Grid

3.2.3.7 Test case of combining Wind, Battery, and Grid

Fig. 31 depicts the results of combining Wind, Battery, and Grid, it shows that the Grid complements the remaining power to fulfill the load on off-peak duration while the battery shares the Grid to complement the missing power for satisfying the demand requirements.

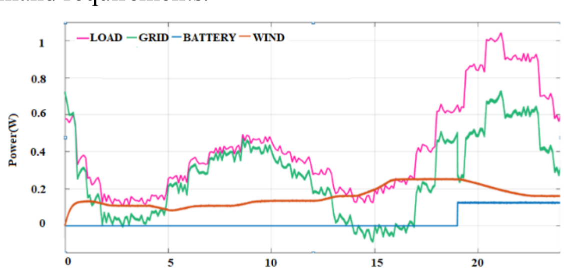

Fig. 31 Experimental test case of combining Wind, Battery, and Grid

3.2.3.8 Comparison between all HRES combination as regard Grid power consumption and exporting

Fig 32 charts the statistics i.e minimum, maximum, mean, median, and standard deviation (STD) of the Grid power of all experimental test cases of combinations of HRES components. Also, Fig. 33 compares the Grid power curves of all HRES combinations, they show that the combination of PV, Wind, Battery, and Grid and that consists of PV, Wind, and Grid is the best in exporting power to the Grid and the first combination is the least one as regard to Grid power consumption. Besides, it shows that the worst combination as regard to the grid power consumption is the combination of PV and Grid.

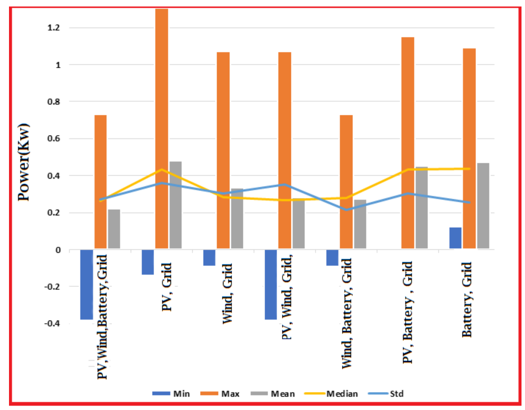

Fig. 32 Experimental results in a statistical comparison of grid Power of all HRES components combinations

Conclusion

By reviewing hundreds of recent researches and last official status reports of HRES, it is concluded that wind and solar energy have the largest growth rate and highest installation capacity. Besides, combining them in a hybrid topology can increase the overall efficiency. So, this paper presents a generic model of HRES including solar PV, novel WTE, and battery. the new WTE has a GUI interface, SQLITE database of the wind turbine as a repository of all related information like wind turbine physical attributes i.e. diameter, tower height, number of blades, axis orientation, and optimum TSR for every wind speed. Therefore, the proposed HRES model is generic and can assess the performance of HRES in a wide range of wind turbine configurations. Besides, it presents a novel MPPT method based on the integration of binary search and particle swarm algorithms to maximize the extracted power of wind and solar energy sources. Furthermore, it introduces the original optimization technique based on GA to optimize the utilization of the generated power based on economical and environmental requirements with considering the system's reliability. the paper presents simulation results and experimental results of different operating conditions including fixed and variable cases of temperature, irradiance, and wind speed. Furthermore, real-time operating conditions of 24 hours have been tested by using a load, temperature, wind speed, and irradiance real profile. The tests include all combinations of HRES components. The simulation and experimental results came in line and showed significant improvement in energy utilization thanks to the proposed energy management technique. And it determined the combination of solar PV, Wind, and Battery is the optimum as regard power generation. furthermore, considering the battery as much as possible is the optimum operation for environmental consideration while using the battery only during on-peak time is recommended for the case of economical optimization. To sum up, this paper introduced and validated a new technique for optimizing and managing the utilization of the generated power of HRES that interprets the economic and environmental operation needs to the optimum share of each component of the HRES.

References

[1] International electricity agency report 2019 http://www.iea.org
[2] Renewables 2019 Global status report http://www.ren21.net/
[3] Y. Abu Eldahab, A. Zekry, N. Saad, Enhancing the Optimization of Hybrid Renewable Energy Systems by Using Statistical Calculations and Data Mining Analysis, IJRER, Vol 9, No 2 (2019), PP 868-886
[4] A. Kaviani, G. Riahy, S. Kouhsari. Optimal design of a reliable hydrogen-based stand-alone wind/PV generating system, considering component outages. Renewable Energy 2009;34(11):2380–90.
[5] A. Chauhan, R. Saini. A review on integrated renewable energy system based power generation for standalone applications: configurations, storage options, sizing methodologies, and control. Renewable Sustainable Energy Rev 2014;38:99–120.
[6] A. Maleki, A. Askarzadeh. Optimal sizing of a PV–wind-diesel system with battery storage for electrification to an off-grid remote region: a case study of Rafsanjan, Iran. Sustainable Energy Technol Assess 2014;7:147–53.
[7] Y. Katsigiannis, P. Georgilakis, E. Karapidakis. Hybrid simulated annealing —Tabu search method for optimal sizing of autonomous power systems with renewables. IEEE Trans Sustainable Energy 2012;3(3):330–8.
[8] A. Menshsari, M. Ghiamy, M. Mousavi, H. Bagal. Optimal design of hybrid water and wind-solar system based on hydrogen storage and evaluation of the reliability index of the system using an ant colony algorithm. Int Res J Appl Basic Sci 2013;4(10):3582–600.
[9] B. Tudu, S. Majumder, K. Mandal, N. Chakraborty. Optimal unit sizing of stand-alone renewable hybrid energy system using bees algorithm. In: IEEE international conference on energy, automation, and signal (ICEAS), 2011; pp. 1–6.
[10] J. Liang, A. Qin, P. Suganthan, S. Baskar. Comprehensive learning particle swarm optimizer for global optimization of multimodal functions. IEEE Trans Evol Comput 2006;10:281–95.
[11] Y. Katsigiannis, P. Georgilakis, E. Karapidakis. Hybrid simulated annealing —Tabu search method for optimal sizing of autonomous power systems with renewables. IEEE Trans Sustainable Energy 2012;3(3):330–8. 200-Askarzadeh A. A discrete chaotic harmony search-based simulated annealing algorithm for optimum design of PV/wind hybrid system. Sol Energy 2013;97:93–101.
[12] A. Abdelkader, A. Rabeh, D. Mohamed, J. Mohamed, Multi-objective genetic algorithm based sizing optimization of a stand-alone wind/PV power supply system with enhanced battery/ supercapacitor hybrid energy storage, / Energy 163 (2018) 351-363, https://doi.org/10.1016/j.energy.2018.08.135
[13] A. Al-Badi. Hybrid (solar and wind) energy system for al Hallaniyat island electrification. Int J Sustain Energy 2011;30:212–22.
[14] J. Kaldellis, D. Zafirakis, K. Kavadias. Minimum cost solution of wind-photovoltaic based stand-alone power systems for remote consumers. Energy Policy 2012;42:105–17
[15] A. Zekry, A. Shaker, M. Salem, Advances in Renewable Energies and Power Technologies, Solar and Wind Energies, 2018, 1:3:56.
[16] M. Wolf, G. Noel, and R. Stirn, "Investigation of the double exponential in the current-voltage characteristics of silicon solar cells," IEEE Transaction on Electron Devices, vol. 24, no. 4, pp. 419-428, Apr.1977.
[17] Y. Abuldahab, N. Saad, A. Zekry. Enhancing the maximum power point tracking techniques for photovoltaic systems. Renew Sustain Energy Rev 2014;40:505–14.
[18] T. Tafticht, K. Agbossou, M. L.Doumbia, A.Che'riti. An Improved Maximum Power Point Tracking Method for Photovoltaic Systems. Renewable Energy 2008;33:1508–1516.
[19] A. Abdelkafi, L. Krichen. New strategy of pitch angle control for energy management of a wind farm. Energy 2011;36:1470–9.
[20] K. Mandal, S. Mandal, B. Bhattacharya, B., N. Chakraborty, "Non-convex emission constrained economic dispatch using a new self-adaptive particle swarm optimization technique", Applied Soft Computing, vol. 28, pp. 188-195, 2015.
[21] H. Yang, L. Lu ,W. Zhou. A novel optimization sizing model for hybrid solar-wind power generation system. Solar Energy 2007; 81: 76–84.
[22] H. Yang, Z. Wei , L. Chengzhi. Optimal design and techno-economic analysis of a hybrid solar-wind power generation system. Applied Energy 2009; 86(2): 163–169.

[23] A. Harrouz; I. Colak; K. Kayisli, Energy Modeling Output of Wind System based on Wind Speed, 2019 8th International Conference on Renewable Energy Research and Applications (ICRERA)
[24] E. Bekiroglu; M. Duran , Analysis of Grid Connected Wind Power System, 2019 8th International Conference on Renewable Energy Research and Applications (ICRERA)
[25] E. Meşe; A. Bakbak; M. Ayaz; M. Boztepe; M. Altıntaş; Ö. Akın; H. Tayyer, Development of Doubly-Fed Direct Drive Modular Permanent Magnet Wind Generator, 2019 8th International Conference on Renewable Energy Research and Applications (ICRERA)
[26] F. Ayadi; I. Colak; N. Genc; H. Ibrahim, Impacts of Wind Speed and Humidity on the Performance of Photovoltaic Module, 2019 8th International Conference on Renewable Energy Research and Applications (ICRERA)

[27] K, Wijesinghe, Optimized Integration of Solar PV Energy on to Telecom Power Systems for DC and A/C buses or Energy Storages with proposed Converters to make them as profit centers 2019 8th International Conference on Renewable Energy Research and Applications (ICRERA)